



# Solutions to hazardous wastes issues in the leather industry: adsorption of Chromium iii and vi from leather industry wastewaters using activated carbons produced from leather industry solid wastes

Jennifer Jimenez-Paz<sup>a</sup>, Juan José Lozada-Castro<sup>b</sup>, Edward Lester<sup>c,\*</sup>, Orla Williams<sup>c</sup>, Lee Stevens<sup>c</sup>, Juan Barraza-Burgos<sup>a</sup>

<sup>a</sup> School of Chemical Engineering, Universidad del Valle, AA 25360 Cali, Colombia

<sup>b</sup> Faculty of Exact and Natural Sciences, University of Nariño, Pasto, Colombia

<sup>c</sup> Faculty of Engineering, University of Nottingham, Nottingham NG7 2RD, UK

## ARTICLE INFO

Editor: P Fernández-Ibáñez

### Keywords:

Leather industry waste

Adsorption

Chromium

Circular economy

## ABSTRACT

This study presents the use of an innovative material to tackle hazardous wastes in the leather industry. Activated carbons produced from Leather industry waste (LIW) were used to adsorb (Cr) III and (VI), which are found in leather wastewater. Two physical and chemical activation processes were used in this study. In physical activation, carbonization and activation with CO<sub>2</sub> were carried out consecutively without intermediate cooling at 700 °C with a residence time of 30 min. In the chemical activation, the LIW was impregnated with a KOH solution in a KOH/LIW ratio of 4/1 w/w. Carbonization was conducted in nitrogen, using two carbonization temperatures, 500 and 700 °C, for 30 min. All activated carbons had Cr (III) adsorption greater than 95%. The experimental data was analysed using Langmuir and Freundlich isotherms. Cr (III) and Cr (VI) adsorption kinetics studies were also carried out based on the Pseudo-first order, Pseudo-second order, Elovich and Intra-particular Diffusion models. The Langmuir and Temkin Isotherm models presented the best fit for Cr (III) adsorption, while the DRK Isotherm models fitted the experimental data for Cr (VI). The thermodynamic parameters of Cr (III) and Cr (VI) adsorption were also determined. A Cr (III) and Cr (VI) adsorption mechanism is proposed using activated carbons from gravel as adsorbent. The production of activated carbon from LIW and its application for the removal of chromium present in the liquid residues of the leather industries can present a potential for the reduction of treatment costs and the application of a circular economy.

## 1. Introduction

The leather production process creates large volumes of solid and liquid waste [1]. Part of the processing, tanning, protects leather against microbial degradation, heat, sweat and moisture [2]. Chromium (Cr (III)) salts are the most widely used tanning agents as it offers excellent hydrothermal stability, better dyeing characteristics, and softness to the leather [3]. However, Cr tanning produces large quantities of liquid and solid Cr-based waste, which have a negative impact on the environment, as well as high waste treatment costs [4]. Circular economy approaches to solid and liquid wastes from the leather industry have the potential to significantly reduce the quantity of wastes and enable Cr recovery [5].

The Colombian leather industry produces approximately 3324 tons of tanned leather annually, distributed around 12 states and 677

tanneries [6]. The highest production comes from Cundinamarca and Antioquia regions. The tanning process uses trivalent chromium sulphate salts (Cr(OH)SO<sub>4</sub>) which bond to the proteins, primarily collagen, of the skin or hide forming a complex [7]. Cr tanning is the most widely used tanning process, as it is less time consuming and produces a high-quality product compared to vegetable tanning [8-10]. However, the treatment of tannery waste has always been a serious issue for leather manufacturers due to the volume and diversity of waste produced, as well as the complex chemical content and high water content of the waste [11]. Processing of one metric ton of rawhide produces on an average 200 kg of tanned leather, 200 kg tanned waste leather, 250 kg of non-tanned waste, and 50,000 kg of wastewater [12]. In Official Development Assistance (ODA) countries such as Colombia, landfilling is the predominant method of dealing with solid tannery waste

\* Corresponding author.

E-mail address: [edward.lester@nottingham.ac.uk](mailto:edward.lester@nottingham.ac.uk) (E. Lester).

<https://doi.org/10.1016/j.jece.2023.109715>

Received 12 October 2022; Received in revised form 10 March 2023; Accepted 15 March 2023

Available online 17 March 2023

2213-3437/Crown Copyright © 2023 Published by Elsevier Ltd.

<http://creativecommons.org/licenses/by-nc-nd/4.0/>.

This is an open access article under the CC BY-NC-ND license

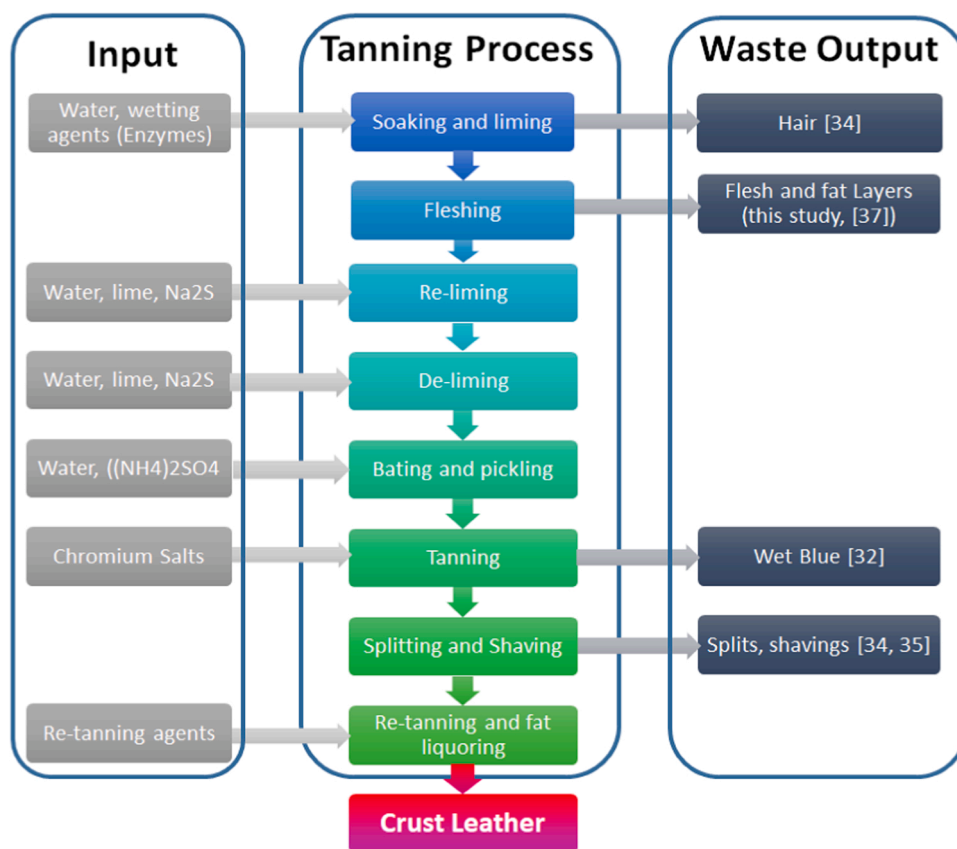


Fig. 1. Tannery process with identified waste outputs used in this and previous studies. Kantarli, Yanik (\$year\$) [55,54,52,57].

treatment [13,6,4]. There is a need for low cost localised sustainable solutions to the leather waste issue in Colombia, which are often small and medium enterprises [14], which can utilise wastes to treat Cr pollution through a circular economy approach.

Cr is a transition Group 6 metal and is the seventh most abundant element in the earth's crust [15]. The most stable valence states are Cr (III) and Cr (VI), with each valence state presenting different chemical and biological properties [16-18]. While Cr (III) is the dominant form of Cr released from the chrome tanning process [19], it is possible for manufacturing steps to possess residual oxidizing functionality capable of converting Cr (III) in the leather to Cr (VI) [20]. Hexavalent Cr (VI) is 500–1000 times more toxic than Cr (III) and causes serious health effects in humans, such as irritation to the skin, kidney and liver, and risk of cancer in respiratory organs and digestives [21-23]. Between 30% and 50% of the incoming Cr (III) salts are generally wasted during the tanning process and end up in the effluent waters or in the sludge in concentrations over 3000 ppm [24,25].

In rivers adjacent to the tanneries in southwestern Colombia, the concentration of Cr (VI) is 26.4 mg/L [26], higher than the permissible limit of 1 mg/L. According to [27], the health effects of Cr(VI) related to concentrations commonly detected in drinking water are still being evaluated, although a link to stomach cancer has been documented. Low-level exposures and chronic exposures are associated with carcinogenic effects in both humans and animals. In addition, a study conducted in southwestern Colombia demonstrated that the main cause of cancer is malignant stomach tumors [28]. This motivates us to consider Cr as a contaminant that must be removed from the water waste from the leather industry.

Adsorption has proved to be an attractive treatment technique for Cr (III) and (VI) in wastewaters based on its low cost, simplicity of operation and the potential to recycle the adsorbent [29,24,30,31]. Activated carbon (AC) is a low cost and non-toxic material which is considered as

an adsorbent for pollutant removal due to its high surface area and porous structure [31,32]. AC adsorption is influenced by solution pH, solution concentration, contact time, temperature, adsorbent dosage, and adsorbent particle size as well as the method of activation of the adsorbent [33]. During AC production, there are several conditions that can affect the physical and chemical properties of the final activated carbon obtained [34]. The type of activating agent will affect the type of porosity and the functional groups on the surface. The activation temperature, heating rate, and residence time between the activating agent and the surface are related to the release of volatile material and therefore to the development of the porosity of the activated carbons. In general, the final properties developed will be the result of the set of operating conditions applied [35].

Commonly used methods to reduce the Cr concentration are ion exchange on polymeric resins, coagulation-flocculation, and reduction/chemical precipitation/sedimentation [36]. These methods require high energy consumption, some of them produce a large amount of sludge and the precipitated chromium is not recovered, increasing the cost of the process [37]. The adsorption of metals in solids represents an economical and efficient method to remove heavy metals present in wastewater. Therefore, there has been great interest in developing economical, efficient, and environmentally friendly adsorbents, among them eggshell, powdered marble, corn residues, algae, almond shells and activated carbons obtained from this type of material. Batch removal percentages of Cr close to 99% and adsorption capacities of the order of 400 mg/g have been obtained [8,38-41,10]. [42] used rice husk and palm leaf to adsorb copper II, cobalt II and iron III ions in batch solution. The results showed the formation of metallic complexes between the bio-adsorbent and the metallic ions. Other bio adsorbents such as palm residues, bagasse have been used for the removal of heavy metals taking advantage of adsorption [43].

There are different variables involved in the chromium adsorption



Fig. 2. (a) Original LIW as received, (b) degreased LIW.

process, among them are the pH of the solution, agitation, adsorbate/adsorbent ratio, temperature, contact time, among others. [44] evaluated the kinetics of chromium III adsorption in marl stones and concluded that the adsorption depends on the adsorbate/adsorbent ratio and that at pH between 2 and 4 the highest adsorption capacity is obtained. A higher dose of adsorbent increases the chromium removal efficiency due to a higher availability of active sites, but the adsorption capacity of the adsorbent decreases due to competition from existing active sites on the adsorbent surface (H. [45]). Regarding the agitation of the solution, [46] obtained greater removal of chromium VI by increasing the agitation speed, because the thickness of the boundary layer on the adsorbent surface is decreased.

Regarding the desorption of the adsorbate on the surface of the activated carbons and subsequent activation, there are different methods proposed. For the desorption of heavy metals on bio-adsorbents, the use of acid solutions ( $H_2SO_4$  or  $HCl$ ) and a subsequent reactivation with a 1 M  $CaCl_2$  solution is found [47,48]. Vinodhini, Das (\$year\$) [49], used a 2 N  $NaOH$  solution to regenerate a Cr (VI) activated carbon. During desorption, part of the Cr (VI) was reduced to chromium III. The main factors for choosing the eluents and the regenerative agent depend on the type of adsorbent and the adsorption mechanism [50]. As a result of the desorption process with 3 activated carbon regeneration cycles, a gradual deterioration of the adsorbent occurs.

The application of activated carbon increases the cost of the treatment process [51]. For this reason, it is necessary to use direct processing wastes to produce activated carbon sorbents, such as leather wastes [52]. Only limited number of studies have been conducted on producing ACs from leather wastes. There are several different wastes from the tanning process which can be used to make activated carbons (Fig. 1). Leather shavings are a residue from the final stage of tanning, and can contain a combination of Cr, vegetable tanned wastes and small pieces of leather [53]. ACs made from leather shavings have shown

adsorption capacities of 57.71 mg/g of Cr (VI), and also removed 78% of Cr (III) from tanning effluent [54]. Chromium and vegetable tanned leather shaving wastes have also been used to make AC for Cr (VI) removal [55], with adsorption capacities higher than that of most of lignocellulosic material-derived activated carbons found in literature. To date, only one other study looks at fleshing wastes, which is an abundant protein source are disposed in large quantity as a solid tannery wastes [56]. Fleshing wastes were used to make activated carbons for removing Cr (VI), with a maximum adsorption capacity of 60.8 mg/g [57]. None of the studies to date explore the potential of direct activation, as they all include a pre-carbonisation stage.

This study explores using LIW from the fleshing stage of the leather production process to produce AC for Cr (III) and Cr (VI) removal as a circular economy solution to two waste issues in the Colombian leather industry. The study is the first to explore potential reductions in energy consumption via a single physical activation step for LIW AC production. Furthermore, the study is the first to explore the potential of using KOH as an activating agent in chemical adsorption. The ACs produced at different temperatures and residence times from a LIW generated in a leather industry were analysed and evaluated to assess their Cr (III) and Cr (VI) adsorption potential. Therefore, the novelty of this study focuses on the use of waste from the leather industry (LIW) and its application as an adsorbent for the adsorption of Cr (III) and Cr (VI), in addition, the novelty of the study includes the activation processes applied (physical and chemical). For physical activation, a direct activation not previously used in the preparation of activated carbons from leather residues was proposed. For chemical activation the KOH activating agent used had not previously been used in the activation of waste leather. The objectives of this work were to study the adsorption kinetics, adsorption equilibrium models, and thermodynamics of the adsorption of Cr (III) and Cr (VI) processes using ACs from LIW as adsorbents.

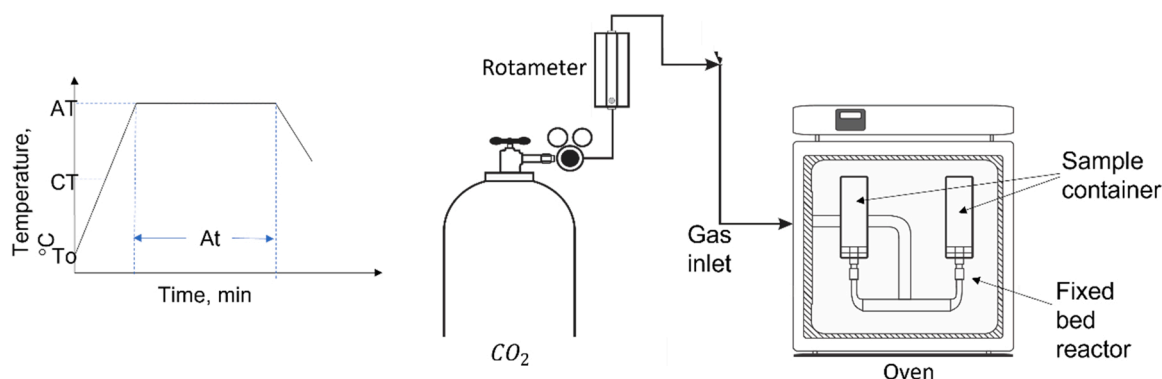


Fig. 3. Schematic of the physical activation processes.

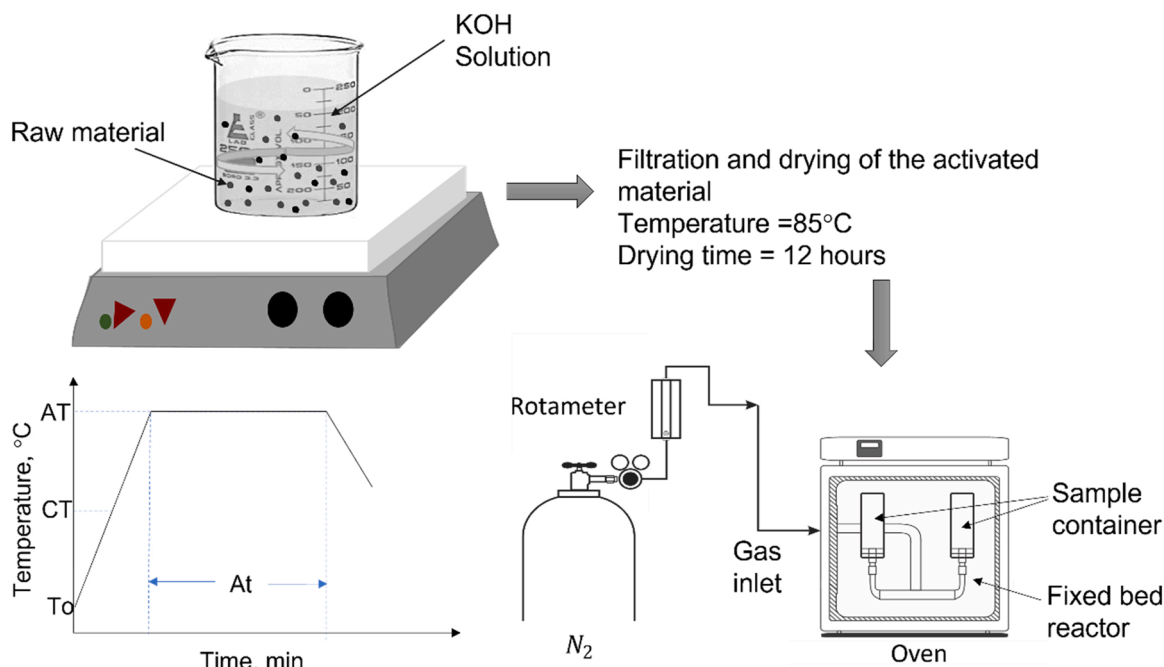


Fig. 4. Schematic of the chemical activation processes.

## 2. Experimental

### 2.1. Reagent and materials

Chemicals and reagents used were of high-purity grade. Stock solutions of Cr (VI) and Cr (III) were prepared using solid  $K_2Cr_2O_7$  and  $Cr_3(OH)_2(OOCCH_3)_7$  then dissolved in demineralized water. The initial pH of the solutions was equal to 5.0 and was adjusted by adding NaOH and HCl solutions before adding the adsorbents and starting the adsorption process.

### 2.2. Leather Industry Wastes

Leather Industry Waste (LIW), as shown in Fig. 2a, was obtained from a tannery in city of Belén, located in the South-western district Nariño in Colombia. LIW originates from the skinning or fleshing stage of the tanning process and contains fat, meat particles and skin particles, as illustrated in Fig. 2. Fat was removed from the LIW through a steam extraction process, using a mixture of the solvents: hexane and isopropanol in a ratio of 5/1 w/w. The LIW does not contain any chromium. The degreased LIW was pulverized to a particle size between 0.85 and 2 mm in a ball mill (Fig. 2b). The degreasing was carried out prior to the activation to increase the concentration of collagen within the LIW.

### 2.3. Activated Carbon Production

Two physical and chemical activation processes were used in this study. To obtain the activated carbons, the activation was carried out with 3 replicates. In physical activation (Fig. 3), carbonization (release of volatile material) and activation with  $CO_2$  were carried out consecutively without intermediate cooling. This reduced energy consumption during the process. Activation temperature and residence time were  $700\text{ }^\circ\text{C}$  and 30 min, respectively. The variables evaluated during the physical activation process were the flow of  $CO_2$  as activating gas (170 and 340 ml/min and the heating rate (5 and  $10\text{ }^\circ\text{C}/\text{min}$ ).

In the chemical activation (Fig. 4), the LIW was dried at  $100\text{ }^\circ\text{C}$  for 1 h, then impregnated with a KOH solution in a KOH/LIW ratio of 4/1 w/w. The impregnation consisted of keeping the LIW in the solution with constant stirring for 1 h, followed by filtration and drying of the

sample for 12 h at  $85\text{ }^\circ\text{C}$ . The impregnations were carried out using a KOH concentration of 3% and 5% w/w. The impregnation ratio was chosen considering previous works on biomass activation [58]. After obtaining the LIW sample impregnated with KOH and dried, carbonization was carried out in an inert atmosphere with nitrogen, using two carbonization temperatures, 500 and  $700\text{ }^\circ\text{C}$ . The variables of operation, residence time and heating rate were kept constant at 30 min and  $10\text{ }^\circ\text{C}/\text{min}$  respectively.

### 2.4. Characterization of the original LIW and activated carbons produced

The LIW was characterized by ultimate analysis in accordance with the standard ASTM D5373 [59]. The surface area and the textural properties of the LIW and the activated carbons produced were characterized by nitrogen and  $CO_2$  adsorption at 77 K and 273 K respectively using an ASAP 2420 V2.09 equipment and MicroActive v5.0 software. To avoid any contaminants, the samples were degassed under vacuum for 15 h at a temperature of 413 K before measurements. The specific surface area was determined using the BET model. The total pore volume and pore size distribution were established using the 2D-NLDFT model for carbons with heterogeneous surfaces [60].

Surface morphologies of the original LIW and activated carbons was observed with Scanning Electron Microscope (SEM) technique, using a Cressington 108 coater with a gold sputtering device. The qualitative estimation of the surface chemistry of the LIW and the activated carbons was carried out using the Fourier transform infrared (FTIR) spectra in the range  $4000\text{--}350\text{ cm}^{-1}$  with a Jasco 4100 instrument using the potassium bromide (KBr) wafer method. Point of Zero Charges (PZC) was determined for activated carbons. 0.150 g of adsorbent was weighed and added to 0.01 M NaCl solutions with different values of pH. The pH of the solutions was adjusted with 0.1 M solutions of HCl and NaOH. Activated carbon in the solution was stirred at room temperature for 48 [61,62].

### 2.5. Batch equilibrium experiment

Cr (III) and Cr (VI) solutions with deionized water at  $20 \pm 1\text{ }^\circ\text{C}$  and  $C_{14}H_{23}Cr_3O_{16}$  and  $K_2Cr_2O_7$  were used in the activated carbon adsorption. The chemicals were reagent grade. Also, NaOH and HCl

solutions were used for pH control during adsorption. Batch adsorption tests were performed in sterile 100 ml disposable polypropylene containers. Synthetic Cr (III) and Cr (VI) solutions were prepared using deionized water for dissolution.

Adsorption tests were performed to determine the best activated carbon for equilibrium and kinetic studies. For this, solutions of 40 ppm for each adsorbate, Cr (III) and Cr (VI), 30 mg of activated carbon was added to 50 ml of solution and the samples were shaken on an orbital shaker (Orbital-Genie Ratcheting Clamps, Scientific Industries) at 210 RPM for 36 h; each experiment was carried out with replication.

The total chromium concentration was determined indirectly according to the procedure described in ASTM D1687 [63], which contains a method for the determination of total chromium by atomic absorption. The quantitative determination of Cr (III) and Cr (VI) in the samples was carried out by measuring their absorbance in a flame atomic absorption equipment (AAAnalyst 100, Perkin Elmer) and comparing the result with a previously prepared calibration curve. Inductively Coupled Plasma Optical Emission Spectroscopy (5110 ICP-OES, Agilent) was used to measure the absorbance of samples with chromium concentrations below 1 mg/L. Before each measurement, the samples were filtered using a 5  $\mu\text{m}$  membrane and then a 0.45  $\mu\text{m}$  membrane to eliminate impurities that could interfere with the absorbance reading. This procedure was repeated for the equilibrium and adsorption kinetics analyses.

The removal percentage (% R) of Cr (III) and Cr (VI) was evaluated by Eq. 1.

$$\%R = \frac{(C_o V_o - C_e V_e)}{C_o V_o} * 100 \quad (1)$$

Where  $C_o$ ,  $C_e$  represent the initial and equilibrium concentration (mg/l) of Cr (III) and Cr (VI) and  $V_o$  and  $V_e$  the initial and equilibrium volume of solution (l).

## 2.6. Batch kinetic experiments

The kinetic adsorption studies were carried out with 50 ml of each Cr (III) and Cr (VI) solution and an initial concentration of 40 ppm. Two temperatures were evaluated, 295 and 308 K. The samples were shaken on heating plates (Stuart *digital undergrad*) to maintain a constant temperature during the test, taking, 0.4 ml aliquots at different time intervals for 5 h. The tests were carried out in duplicate. For each sample taken, the amount of chromium adsorbed in equilibrium per gram of activated carbon was measured using Eq. 2:

$$q_e = \frac{(C_o V_o - C_e V_e)}{M} \quad (2)$$

Where,  $q_e$  is the mass of solute adsorbed at equilibrium per gram of adsorbent, mg/g;  $C_o$  is the initial concentration, mg/l;  $C_e$  is the steady-state concentration, mg/l;  $V_o$  is the initial volume of solution, l;  $V_e$  is the volume of the solution at equilibrium, l and  $M$  is the activated carbon mass, g.

Selectivity between Cr (III) and Cr (VI) in the activated carbons produced was studied. It was determined by the distribution coefficient,  $K_d$ , calculated with Eq. 3[64,65]:

$$K_d = \frac{C_o V_o - C_e V_e}{C_e} \left( \frac{1}{M} \right) \quad (3)$$

## 2.7. Adsorption isotherms

Adsorption isotherms were determined to study the equilibrium adsorption phenomenon. 30 mg of activated carbon were added to the solutions of Cr (III) (initial concentrations of 40, 89, 120, 240, 360, 480 and 600 mg/l) and Cr (VI) (initial concentrations of 6, 8,12,24,40,120 mg/l). The initial volume of the solutions was 50 ml,

**Table 1**

Ultimate analysis of the as received degreased LIW, dry basis, db.

Raw material	Ash, %	C, %	H, %	N, %	S, %	O* %
LIW	5.1	56.8	8.4	8.8	0.3	20.6

\* By difference

and they were shaken on an orbital shaker (Orbital-Genie Ratcheting Clamps, Scientific Industries) at 210 RPM for 36 h. The tests were carried out in duplicate.

## 3. Results and discussion

### 3.1. Characterization of the original LIW

Fig. 2 shows a photograph of the original and degreased LIW. The original LIW of spongy morphology, white colour and low density is observed, in comparison with the degreased LIW that looks more compact and greyer in colour. The ultimate analysis of the degreased LIW, on a dry basis, is presented in Table 1. Nitrogen content is known to play an important role in AC absorbance. Porous carbons doped with nitrogen show greater adsorption capacity for acid adsorbents [66]. Furthermore, increased nitrogen content in ACs promotes the interaction between nitrogen functional groups, which play a key role in AC  $\text{CO}_2$  absorbance, and  $\text{CO}_2$  on the surface of N-doped ACs produced from sugarcane bagasse [67]. Fig. 5 shows the images of the as received LIW from the scanning electron microscope. A slightly inflated, disorderly structure with a very low initial porosity is evident for the LIW.

### 3.2. Mass yields and surface areas of activated carbons

Table 2 shows the mass yields (MY, % w/w on ash-free dry basis, afdb) and the surface areas, (AS),  $\text{m}^2/\text{g}$ , of the LIW activated carbons obtained using physical and chemical activation as a function of activation temperature, residence time, heating rate,  $\text{CO}_2$  flow, and KOH concentration. The nomenclature used to identify the samples is as follows: R1 to R4 are activated carbons obtained by physical activation and RQ1 to RQ4 are chemically activated. It was found that the activated carbons produced by physical activation presented mass yields in the range of 33.5–35.3%, which means that despite the change in operating conditions, no significant changes occurred. The low porosity found in activated carbons ( $2.9\text{--}4.4 \text{ m}^2/\text{s}$ ) could explain this behaviour. As shown in Table 2, it was found that both the surface areas of the original LIW and the activated carbons are small compared to other carbonaceous residues that present surface areas higher than  $100 \text{ m}^2/\text{g}$  [68,58, 69].

The mass yields of the activated carbons produced by chemical activation using a KOH concentration of 3% were higher than those obtained with a concentration of 5% and those obtained by physical activation. It is highlighted that, when chemically activating the LIW, the highest mass yield obtained was 44.6% using the lowest activation temperature ( $500 \text{ }^\circ\text{C}$ ) and the lowest concentration of KOH (3%). The low presence of KOH possibly produces an effect in decreasing the release of volatile matter from the LIW and therefore, the highest mass yields are obtained. Concerning to the surface areas of the activated carbons obtained by physical and chemical activation, it was observed that, in general for all operating conditions, there was an increase in their surface areas compared to that of the original LIW. This suggests that operating conditions had some effect on carbonization and its porosity. It was also found that, during chemical activation, the surface area of activated carbon tends to decrease with increasing activation temperature. It seems that, at higher temperatures, sintering of the surfaces occurs, which causes the porosity of the char to increase.

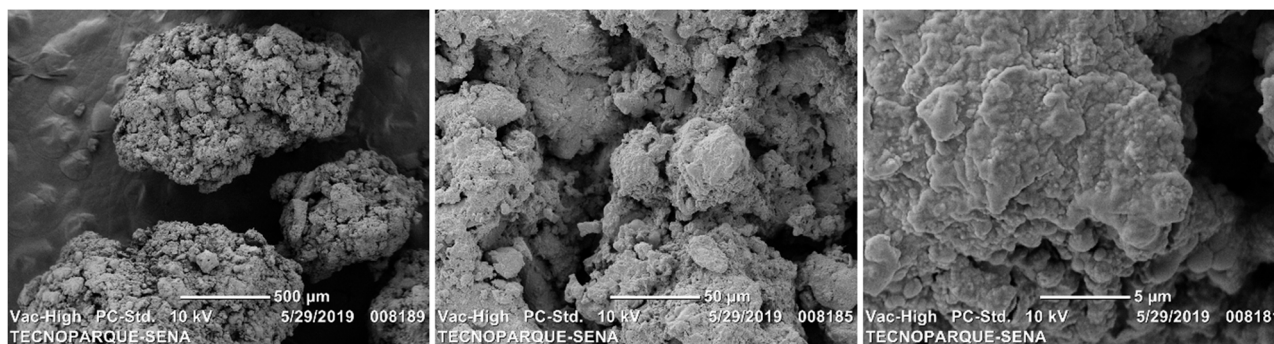


Fig. 5. SEM of as received LIW.

Table 2

Mass yields and surface areas of as received LIW and LIW activated carbons obtained physically and chemically.

Samples	AT, ° C	At, min	HR, ° C/ min	FCO <sub>2</sub> , ml/ min	KOH, % w/w	MY, % w/w	SA, m <sup>2</sup> /g	SD, %
Original LIW	-	-	-	-	-	100	0.124	
Physical activation								
R1	700	30	5	170	-	35.3	2.93	0.70
R2	700	30	5	340	-	34.7	3.87	0.21
R3	700	30	10	170	-	33.5	4.03	1.33
R4	700	30	10	340	-	35.2	4.48	1.11
Chemical activation								
RQ1	500	30	10	-	3	44.6	4.67	1.14
RQ2	700	30	10	-	3	43.5	2.75	1.07
RQ3	500	30	10	-	5	39.9	1.97	1.29
RQ4	700	30	10	-	5	27.2	2.59	0.77

AT, Activation temperature; At, Activation time; HR, Heating Rate; FCO<sub>2</sub>, CO<sub>2</sub> flow; MY, Mass Yield; SA, Surface Area; SS, Standard deviation.

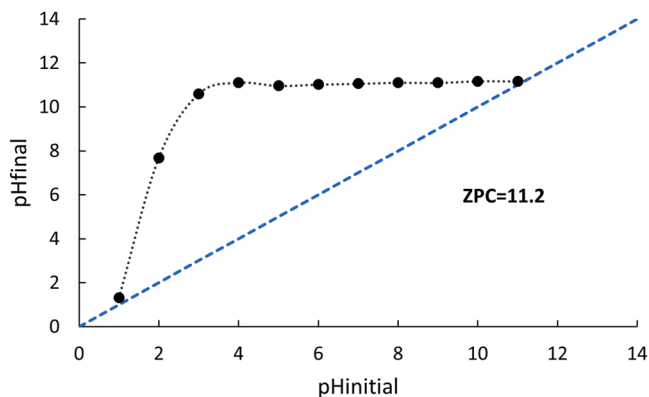


Fig. 6.  $pH_{final}$  vs  $pH_{initial}$  for activated carbon R4.

### 3.3. $pH_{PZC}$ determination

Fig. 6 shows the behaviour of the final pH as a function of the initial pH, the PZC value found was equal to 11.2, higher than the working pH for the adsorption process ( $pH=5$ ), therefore it can be said that the surface of the adsorbent will be positively charged and will favour the adsorption of negatively charged species [65].

### 3.4. FTIR analysis of original LIW and activated carbons

Fig. 7 shows the IR spectra of the LIW and activated carbons R1 to R4, obtained by physical activation and chemical activation. In general, bands were identified at wavelengths 900, 1500, 2900 and 3400. The

peak around  $900\text{ cm}^{-1}$  corresponds to vibrations of aliphatic groups C-C, C-O and C-N, where the original LIW showed less intensity compared to the activated carbons, suggesting that graphitization occurred. The peak at  $1500\text{ cm}^{-1}$  wavelength corresponds to C=C and N=N double bonds. As can be seen, there were no intensity differences in the LIW and activated carbons.

The  $2900\text{ cm}^{-1}$  peak is attributed to the C-H,  $-\text{CH}_2-$  and  $-\text{CH}_3$  aliphatic chains of activated carbons, while the  $3400\text{ cm}^{-1}$  peak corresponds to O-H and N-H vibrations, possibly due to the presence of water and nitrogen compounds. Both peaks show lower intensities in the activated carbons compared to the original LIW, which could be due to increased carbonization.

A notable difference was found between physical and chemical activation. The samples of the chemically activated carbons showed peaks between  $2170$  and  $2235\text{ cm}^{-1}$  corresponding to triple C≡C, C≡O bonds or quite possibly to the C≡N bond due to the high nitrogen content of the LIW. These peaks are not seen in the original LIW or physically activated carbons. Therefore, chemical activation favoured the formation of triple bonds.

### 3.5. Adsorption of Cr (III) and Cr (VI) using artificial solutions

According to the results obtained during the characterization of activated carbons using LIW as raw material, those that presented the two largest surface areas for physical and chemical activation were chosen. Therefore, adsorption tests were carried out to determine the percentage of removal of Cr (III) and Cr (VI) for samples RQ1, RQ2, R3 and R4. Table 3 shows the results of the preliminary adsorption tests.

For Cr (III), the RQ1 sample presented the highest removal percentage (99.42%) and selectivity with a  $K_d$  equal to 283 L/g. This sample also showed the highest surface area among all activated carbons (See Table 2), both those obtained by the physical and chemical processes. In general, for all adsorbents, Cr (III) presented a removal percentage greater than 95%. This is attributed to the strong affinity that the raw material has with Cr (III). Previous adsorption studies [70] reported a similar removal rate of Cr (III), close to 99% for an initial concentration of 100 mg/l, using microalgae as adsorbent. In addition, removal of around 70% of Cr (III) was reported from a solution with an initial 10 ppm of adsorbate and residues of pine nut seeds [71].

Regarding the adsorption of Cr (VI), the original LIW presented the best removal percentage equal to 12.54%, indicating that for this adsorbate the activation does not represent a benefit for the Cr (VI) adsorption process and that the surface area is not a factor. determining as if the functional groups present on its surface can be, such as C≡C, C≡O y C≡N formed during chemical activation. It could be suggested that these functional groups decrease the Cr (VI) adsorption rate, but do not interfere with Cr (III) adsorption.

The percentage of removal of Cr (VI) was lower than those obtained in other studies that use agricultural residues to obtain activated carbon. Murad et al., (Year\$) [72] found that for an initial Cr (VI) solution of

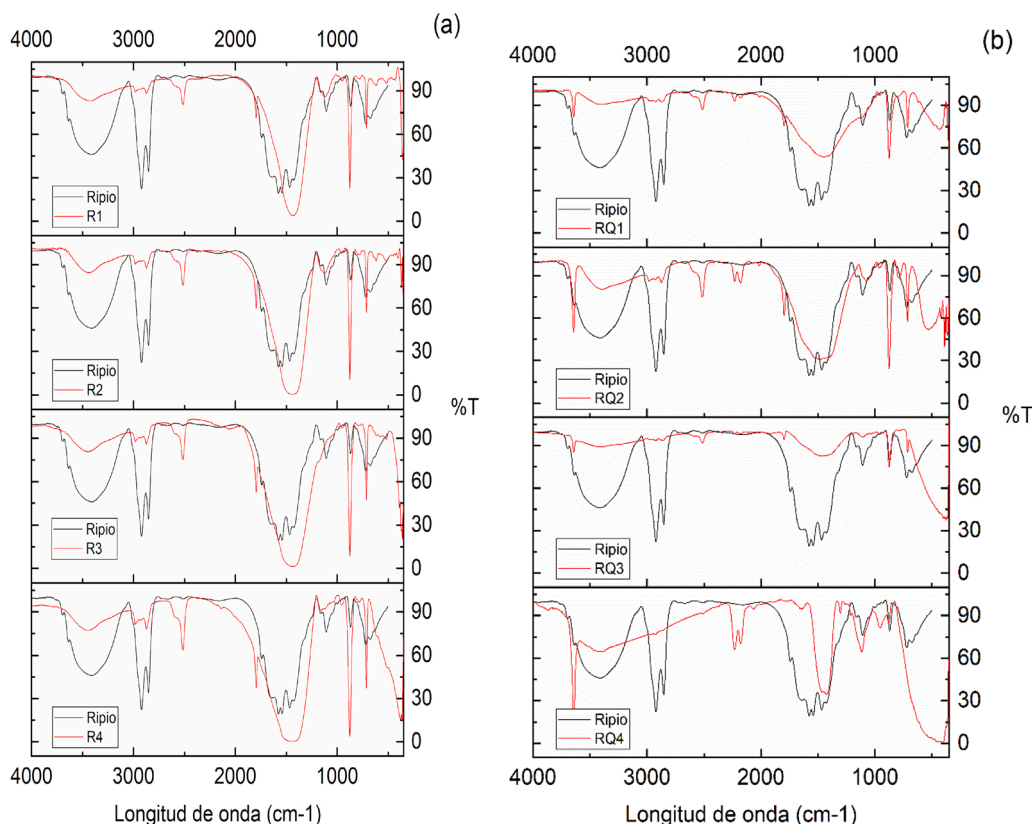


Fig. 7. FTIR of activated carbons obtained by (a) physical activation and (b) chemical activation.

**Table 3**  
Removal of Cr (III) and Cr (VI).

Samples selected	Cr (III)			Cr (VI)		
	Removal, %	SD*	Kd, L/g	Removal, %	SD*	Kd, L/g
LIW	96.17	0.00	41.3	12.54	0.04	0.294
RQ1	99.42	0.00	283	7.39	0.01	0.132
RQ2	98.98	0.01	160	7.87	0.02	0.140
R3	98.85	0.01	141	9.75	0.01	0.176
R4 *	99.13	0.01	188	10.30	0.01	0.189

\*SD: Standard deviation, \* Activated carbon chosen for equilibrium and kinetic studies

40 ppm it obtained a removal greater than 60% using modified peanut shell as adsorbent. (H. [73]) adsorbed about 99% of Cr (VI) using biomass composting and an initial concentration of Cr (VI) in the solution of 8 ppm.

Studies report higher selectivity for Cr (VI) between 2.523 and 0.714 l/g, compared to Cr (III) whose selectivity values range between 0.330 and 0.011 l/g. On the contrary, the present adsorbent has a higher affinity for Cr(III) compared to Cr(VI) due to higher  $K_d$  values obtained for Cr(III) [74].

The important thing about this work is to have crossed the frontier of knowledge in Cr (III) and (VI) adsorption works by using residues of animal origin such as LIW, which has not been reported in the literature. Based on the good performance in the adsorption of Cr (III), activated carbon R4 was chosen to carry out adsorption studies in equilibrium and kinetics.

### 3.6. Equilibrium Isotherms

Activated Carbon R4 was selected for further analysis due to its superior Cr (VI) adsorption compared to the other samples tested. R4 was physically activated at 700 °C for 30 min, with the heating rate of 10 °C/

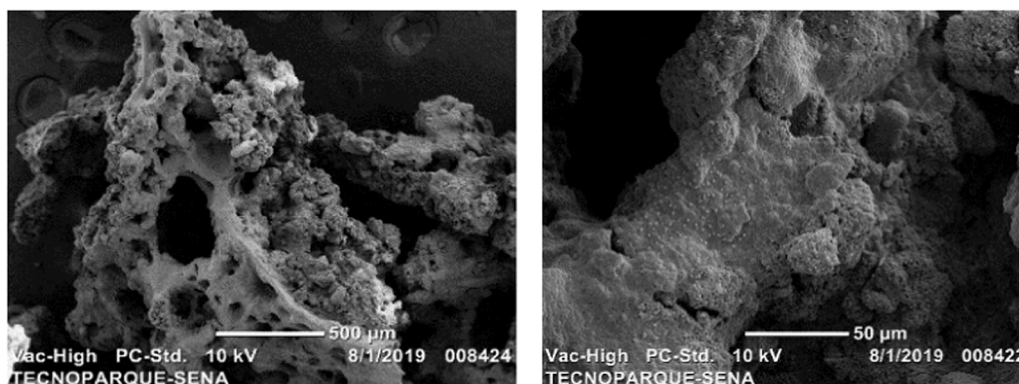


Fig. 8. SEM of Activated Carbon R4 at 500 µm (left) and 50 µm (right) scale.

**Table 4**  
Adsorption parameters for Cr (III) and Cr (VI) for activated carbon R4.

Equilibrium Model	Parameter	Cr (III)	Cr (VI)
Langmuir	$q_{\max}$	220	0
	$b$	0.213	0
	$R_L$	0.105	1.00
	RMSE	21.9	15.0
Freundlich	$k_F$	80.8	0.0588
	$1/n$	0.202	1.40
	RMSE	6.16	1.30
Temkin	$K_t$	11.3	0.112
	B1	29.5	11.5
	RMSE	4.53	5.75
DRK	$X_m$	202	41.6
	$\beta$	7.37e-04	2.69e-04
	RMSE	27.9	0.557

min and 340 ml/min of CO<sub>2</sub> as activating gas. Fig. 8 shows the SEM of R4, which has increased porosity compared to the pre-treated LIW (Fig. 5).

To study the equilibrium adsorption process, Langmuir, Freundlich, Temkin and Dubinin–Kaganer–Radushkevich (DRK) models were applied, which are the most commonly applied adsorption models for chromium adsorption using activated carbons [75-77]. Langmuir's model assumes that the adsorbate is adsorbed in a monolayer that covers the surface of the adsorbent, and the molecule is in an active site present on the surface [77]. The Langmuir isotherm presents a good correlation for a wide variety of experimental data. Langmuir's approach is described by the following equation [78]:

$$q_e = \frac{q_{\max} \cdot b \cdot C_e}{1 + b \cdot C_e} \quad (4)$$

Where,  $q_e$  is the adsorbed Chromium concentration at equilibrium, mg/g,  $C_e$  is the chromium concentration in the equilibrium solution, mg/l;  $q_{\max}$  is the maximum adsorption capacity in a monolayer, mg/g, and  $b$  is the Langmuir equilibrium constant (l/mg). To establish the adsorption advantage through the type of isotherm, the dimensionless equilibrium parameter was determined with Eq. 5:

$$R_L = \frac{1}{1 + b \cdot C_0} \quad (5)$$

where  $b$  is the Langmuir constant and  $C_0$  is the initial concentration of the solution. The value of  $R_L$  indicates the type of isotherm: unfavourable ( $> 1$ ), linear ( $= 1$ ), favourable (between 0 and 1) or irreversible ( $= 0$ ) [79].

The Freundlich equation is an empirical model that considers heterogeneous adsorption energies at the adsorbent surface [80]. It can be applied to non-ideal adsorption on a heterogeneous surface, as well as to

multilayer adsorption. This model does not have a thermodynamic fundamental, since at low concentrations it is not reduced to Henry's law [81]. It is expressed by Eq. 6.

$$q_e = K_f C_e^{1/n} \quad (6)$$

Where,  $K_f$  and  $1/n$  are constants of the Freundlich isotherm.

The Temkin model is applied for those adsorption processes in which the enthalpy of adsorption is inversely proportional to the adsorption capacity and describes adsorbent-adsorbate interactions [82]. The equation is described in Eq. 7:

$$q_e = B_1 \ln(K_t \cdot C_e) \quad (7)$$

$B_1$  is the constant relative to heat of adsorption and is defined by the expression  $B_1 = RT/b$ , with  $b$  being Temkin's constant (J/mol),  $T$  in Kelvin, and  $R = 8.314$  J/mol.K;  $K_t$  is the equilibrium binding constant or thermal constant [83].

The DRK model allows calculating the maximum amounts adsorbed. The behaviour of the adsorption isotherm is like the results of the immersion enthalpy as a function of concentration, for this reason the DRK model is used to determine the energy involved in the adsorption process. The DRK isotherm has the following formula:

$$q_e = X_m e^{-\beta \cdot \varepsilon^2} \quad (8)$$

$$\varepsilon = R \cdot T \cdot \ln \left( 1 + \frac{1}{C_e} \right) \quad (9)$$

Where  $\beta$  is the activity coefficient constant,  $\varepsilon$  is the Polanyi's potential,  $R$  is the gas constant in J/mol.K, and  $T$  is the temperature in Kelvin.

The parameters of the nonlinear isotherm models were calculated by minimizing the mean square error, the parameter values obtained and the respective RMSE for each isotherm model are presented in Table 4.

For Cr (III) adsorption, the lowest RMSE was obtained for the Freundlich and Temkin models. Maximum adsorption capacities above 202 mg/g were obtained for the Langmuir and DRK models. The dimensionless equilibrium parameter  $R_L$ , less than 1, showed that the adsorption process is favourable for Cr (III).

On the other hand, Cr (VI) for the Langmuir model did not show a good fit, since despite having a lower RMSE value compared to Cr (III), the parameters found are not physically consistent. The DRK model presented the best fit for Cr (VI) adsorption with the lowest RMSE value equal to 0.557, a maximum adsorption capacity equal to 41.6 mg/g was calculated using this model. Freundlich model showed an acceptable fit. The value of the parameter  $K_F$  for the Freundlich model is higher for Cr (III) compared to Cr (VI). This parameter is directly related to the adsorption capacity of the adsorbent. Therefore, a higher magnitude indicates that activated carbon adsorbs a greater amount of Cr (III) than Cr (VI), which agrees with the results obtained with the Langmuir and DRK models. Regarding the parameter  $1/n$ , for Cr (III), a value was

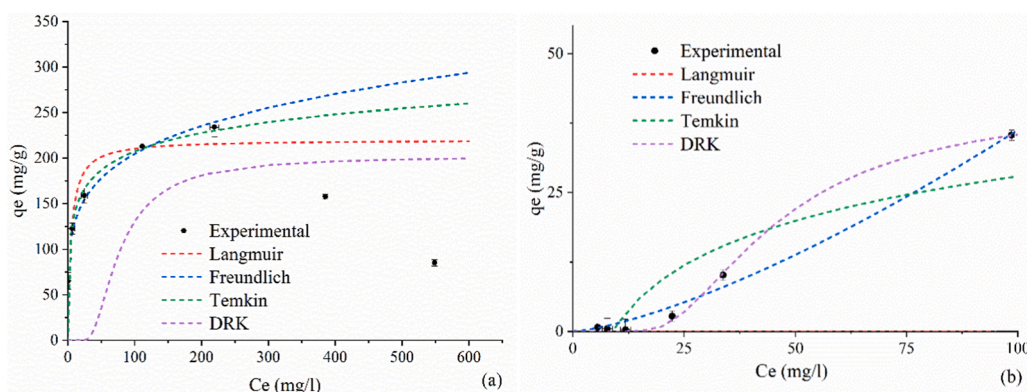


**Fig. 9.** Adsorption isotherm using physically activated carbon. a) Cr (III), b) Cr (VI) for activated carbon R4.

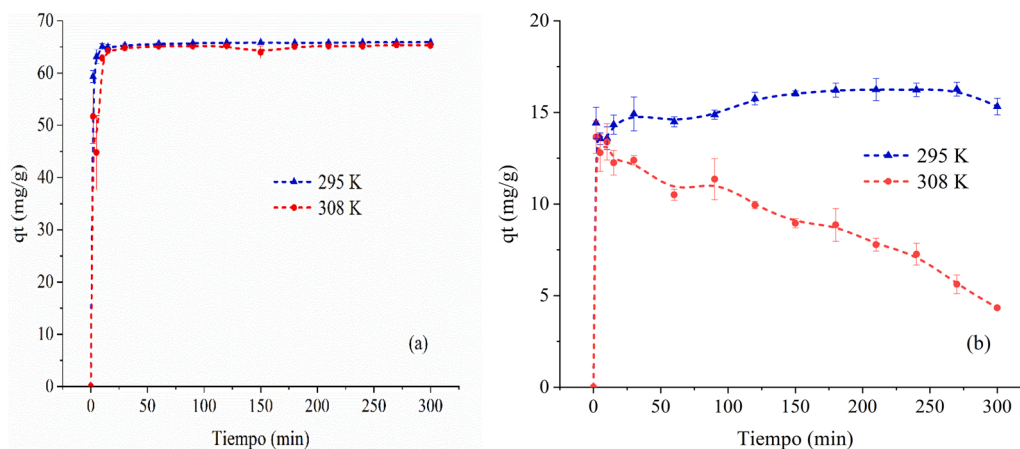


Fig. 10. Cr (III) (a) and Cr (VI) (b) adsorption kinetic for activated carbon R4.

obtained within the range 0 and 1, corroborating the favourability of the adsorption process for this adsorbate. These results agree with those reported by S. Chen et al. (S. [84]).

Fig. 9 shows the relationship between the amount of adsorbate on the surface of activated carbon ( $q_e$ ) and the equilibrium concentration ( $C_e$ ) of the Cr (III) solution for Fig. 9a and Cr (VI) for Fig. 9b. The experimental values of the adsorption isotherms are presented, and the theoretical models are compared. In the case of Cr (III) adsorption, Temkin and Freundlich show a better fit compared to Langmuir y DRK, which may indicate that Cr (III) adsorption is performed at localized sites on the activated carbon surface and in monolayer.

According to the classification of adsorption isotherms in liquid solutions, for Cr (III) a type L isotherm is observed. The initial behaviour of Cr (III) adsorption on activated carbon from the grave is almost vertical, indicating that at low concentrations Cr (III) is completely adsorbed on activated carbon, this behaviour represents a special case of L-type isotherms. Fig. 9a also shows that at equilibrium concentrations greater than 100 mg/l, the slope of the isotherm decreases until reaching a maximum concentration of adsorbate in the activated carbon, which is attributed to the fact that the adsorption capacity is limited by the number of active sites present in the activated carbon. The forces that could be intervening in the adsorbate-adsorbent interaction are weak of the Van der Waals type, revealing possible physical adsorption (Bonilla-Petriciolet, A., Mendoza-Castillo, DI, & Reynel-Ávila, 2017).

Additionally, it was found that at equilibrium concentrations greater than 200 mg/l, a lower concentration of Cr (III) occurred in the activated carbon and the adsorption capacity of the adsorbent was reduced. This could be due to the solute-solute interaction (Cr (III)-Cr (III)), which is stronger than the interaction that occurs between Cr (III) and activated carbon, reducing the amount of adsorbate that reaches the active sites of the adsorbent and adsorption rate. Similar studies [71] reported Cr (III) adsorption capacities between 18 and 22 mg/g using bio adsorbents. Other adsorbents [38] have also been used for the adsorption of Cr (III), such as marble powder and eggshell with adsorption capacities equal to 434.82 and 200.25 mg/g respectively.

Regarding the adsorption of Cr (VI) on activated carbon from LIW, the type of isotherm that resembles the behaviour of the Cr (VI) adsorption process is type S represented by the DRK model with an RMSE value of less than 1, indicating that initially, the interaction between the adsorbate and the surface of the adsorbent is low. However, once the adsorption process begins, there is a better accommodation of the adsorbate molecules, allowing a greater adsorption capacity of Cr (VI) on the activated carbon, it is also hypothesized that the interaction of the adsorbate molecules that already adsorbed, favour interaction with free adsorbate molecules to facilitate their arrival at the surface and active sites of activated carbon [85].

Table 5

Thermodynamic parameters of activated carbon R4.

T (K)	Cr (III)			Cr (VI)		
	$\Delta G$ (kJ/mol)	$\Delta H$ (kJ/mol)	$\Delta S$ (kJ/(mol. K))	$\Delta G$ (kJ/mol)	$\Delta H$ (kJ/mol)	$\Delta S$ (kJ/(mol. K))
295	-12.6	-24.2	-0.039	2.48	-30.8	-0.113
308	-12.1			3.95		

### 3.7. Adsorption kinetic of Chromium II and Cr (VI)

Adsorption kinetic describes the adsorption rate of the adsorbate and models the removal rate of Cr (III) and Cr (VI) for activated carbon R4. Fig. 10 shows the adsorption kinetics of Cr (III) and (VI) at temperatures of 295 K and 308 K. In general, for the two temperatures, the adsorption process of Cr (III) presented higher adsorption (65 mg/g) compared to Cr (VI), which presented less than 20 mg/g.

The process temperature had some effect on the adsorption kinetics. For both adsorbates, it was found that the temperature of 308 K decreases the amount adsorbed on the activated carbon, which possibly indicates that the adsorption energy is exothermic.

With the kinetic data obtained at the two temperatures of the adsorption process, the thermodynamic parameters Gibbs free energy ( $\Delta G$ ), enthalpy ( $\Delta H$ ) and entropy change ( $\Delta S$ ) were calculated, following the procedure described in [86]. The thermodynamic parameters results are shown in Table 5.

$\Delta H$  for both adsorbates was negative, corroborating the aforementioned exothermic behaviour [87]. The absolute value of  $\Delta H$  is greater for Cr (VI) compared to Cr (III). Therefore, an increase in temperature affected the adsorption of Cr (VI) to a greater extent and a decrease in the adsorption capacity of activated carbon was observed. On the contrary, Cr (III) did not present a significant variation with increasing temperature, as can be seen in Fig. 10. The magnitude of  $\Delta H$ , less than 84 kJ/mol, indicates that the type of adsorption presented represents physisorption, which agrees with that reported by S. [84]. Regarding  $\Delta G$ , negative values were presented for the adsorption of Cr (III), indicating the spontaneity of the process. On the contrary, Cr (VI) presented positive results for  $\Delta G$ , revealing that the process is not spontaneous and that some external force is required to favour the adsorption of this adsorbate [88]. The  $\Delta S$  predicts the surface changes of the adsorbent during adsorption. A negative value, as is the case in the present study, reflects that there is no significant change in the internal structure of the adsorbent during adsorption. Furthermore, it could show that during adsorption there is a decrease in disorder at the solid/liquid interface; therefore, there will be molecules that escape from the solid phase to the

**Table 6**  
Kinetic models used to study adsorption kinetics.

Kinetic models	Non-linear equation	Linear equation
Pseudo-primer order	$\frac{dq_t}{dt} = K_1(q_e - q_t)$	$\ln(q_e - q_t) = \ln q_e - K_1/2.303t$
Pseudo-segundo order	$\frac{dq_t}{dt} = K_2(q_e - q_t)^2$	$\frac{t}{q_t} = \frac{1}{K_2 q_e^2} + \frac{t}{q_e}$
Elovich	$\frac{dq_t}{dt} = \alpha e^{-\beta q_t}$	$q_t = \frac{1}{\beta} \ln(\alpha \beta) + \frac{1}{\beta} t$
Intraparticular diffusion	$q_t = f(t^{1/2})$	$q_t = K_{id} t^{1/2} + C$

Where the kinetic parameters  $K_1$  ( $\text{min}^{-1}$ ),  $K_2$  ( $\text{min}^{-1}$ ),  $\alpha$  ( $\text{mg}/(\text{g}\cdot\text{min})$ ),  $\beta$  ( $\text{mg}/\text{g}$ ),  $C$  ( $\text{mg}/\text{g}$ ) and  $K_{id}$  ( $\text{mg}/\text{g}\cdot\text{min}^{-1/2}$ ) are constant.

liquid phase and decrease the amount of adsorbate adsorbed [89]. This phenomenon can be seen in the experimental data reported in Fig. 8a and Fig. 9b.

The models of the adsorption kinetics of Cr (III) and Cr (VI), chosen in this work, were those of Pseudo-first order, Pseudo-second order, Elovich and Intraparticular Diffusion [64,90,91]. In Table 6 the non-linear and linear equations of each model are presented.

Tables 7 and 8 present the characteristic parameters of each

**Table 7**  
Parameters of Cr (III) adsorption kinetic models.

Temperature, K	295			308		
Kinetic models	Parameters		R <sup>2</sup>	Parameters		R <sup>2</sup>
Pseudo-first order	$K_1$ 0.015	$q_e$ 2.01	0.332	$K_1$ 0.284	$q_e$ 30.23	0.191
Pseudo-second order	$K_2$ 0.087	$q_e$ 65.84	1.000	$K_2$ 0.054	$q_e$ 65.36	1.000
Elovich	$\alpha$ 3. E + 20	$\beta$ 0.774	0.725	$\alpha$ 4. E + 33	$\beta$ 1.26	0.781
Intraparticular diffusion	$K_{id}$ 0.439	$C$ 61.91	0.493	$K_{id}$ 0.234	$C$ 62.99	0.662

**Table 8**  
Parameters of Cr (VI) adsorption kinetic models.

Temperature, K	295			308		
Kinetic models	Parameters		R <sup>2</sup>	Parameters		R <sup>2</sup>
Pseudo-first order	$K_1$ 0.041	$q_e$ 3.40	0.546	$K_1$	$q_e$	
Pseudo-second order	$K_2$ 0.059	$q_e$ 15.46	0.998	$K_2$ 0.048	$q_e$ 10.24	0.994
Elovich	$\alpha$ 2. E + 16	$\beta$ 2.86	0.494	$\alpha$ 2. E-08	$\beta$ 1.21	0.808
Intraparticular diffusion	$K_{id}$ 0.163	$C$ 13.59	0.634	$K_{id}$ 0.351	$C$ 13.98	0.854

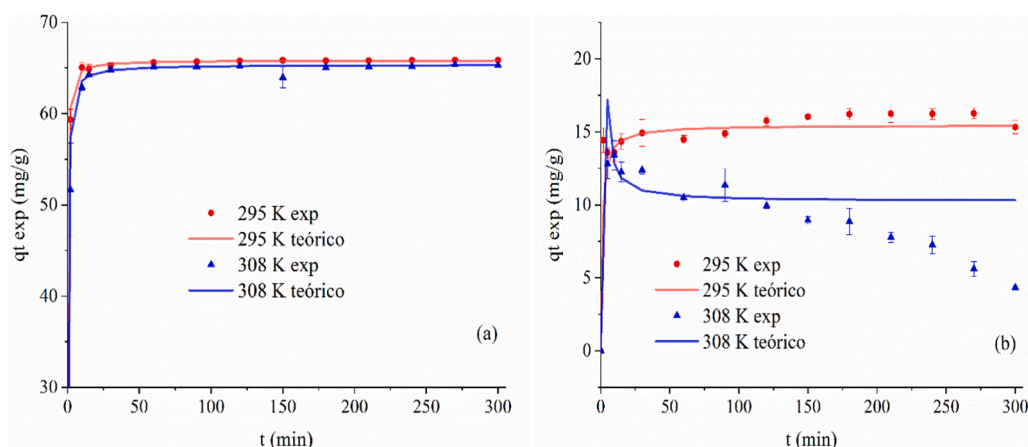


**Fig. 11.** Cr (III) (a) and Cr (VI) (b) adsorbed using the pseudo-second-order kinetic model.

adsorption kinetic model for Cr (III) and Cr (VI) respectively, at the two temperatures, in addition to the correlation coefficients ( $R^2$ ). For both temperatures and adsorption kinetics of Cr (III) and Cr (VI), low correlation coefficients were found for the pseudo-first order, Elovich and intraparticle diffusion models.

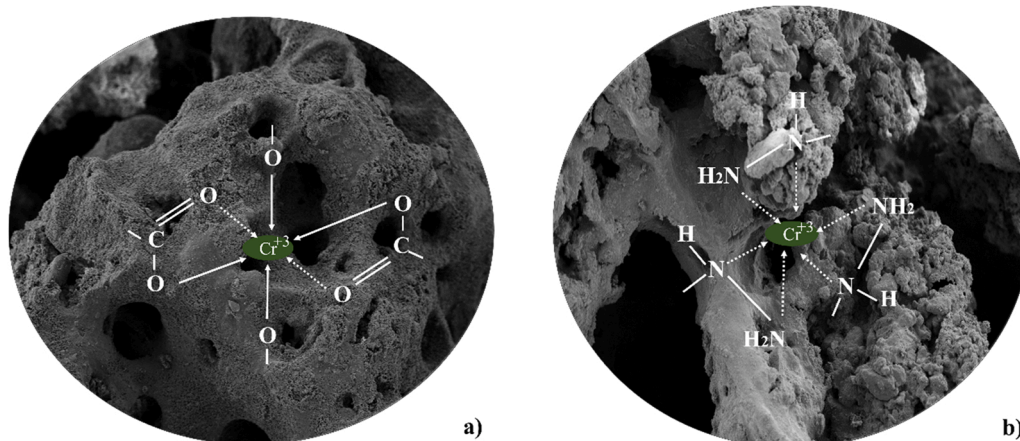
The pseudo-second-order model presented the best regression with the experimental data obtained. The best fit was found with a correlation coefficient of 1.0 for Cr (III) adsorption kinetics, at both temperatures, while 0.998 and 0.994 for Cr (VI) adsorption kinetics. This suggests that the adsorption of Cr (III) and Cr (VI) on activated carbon RQ4 is represented by a pseudo-second-order kinetic model. This model assumes that two reactions occur, the first is fast and reaches equilibrium quickly and the second is a slower reaction that continues for long periods [88]. Another study has shown adsorption kinetics of pseudo-second order for Cr (VI) adsorption using raw materials such as peat, leaf mould, corncob, and granular activated carbon [92,93].

Fig. 11 presents the calculated and experimental values of Cr (III) and Cr (VI) adsorbed against time using the pseudo-second-order kinetic model. The curves indicate that the model is consistent with the experimental data obtained.

In Table 9, a comparison is made of the use of solid waste from the tannery industry for the adsorption of Cr (VI) and Cr (III). The use of solid waste generated in different stages of the tanning process for the adsorption of mostly Cr (VI) is observed, the studies do not focus on the adsorption of Cr (III), the oxidation state used for the tanning of leather skin. The material obtained in the present study was evaluated for the adsorption of both chromium oxidation states, obtaining superior results in the adsorption capacity for Cr (III), this shows the potential that this

**Table 9**  
Comparison to previous LIW Chromium adsorption studies.

LIW used	Stage of the leather process	Treatment	Reference	Adsorption capacity, Cr (VI)	Adsorption capacity, Cr (III)
Hair	Soaking and liming	Physical(steam) activation	Louarrat (\$year\$)[54]	50 mg/g	Not reported. 73% of decrease
Flesh and fat layers	Fleshing	Chemical activation (ZnCl <sub>2</sub> )	Palani et al., (\$year\$) [57]	60.8 mg/g	None
Wet blue	Tanning	Physical (CO <sub>2</sub> ) Activation	Oliveira et al., (\$year\$) [52]	None	None
Leather shavings	Splitting and shaving	Chemical activation (ZnCl <sub>2</sub> and H <sub>3</sub> PO <sub>4</sub> )	Kantarli, Yanik (\$year\$) [55]	126.6–138.9 mg/g	None
Flesh and fat layers	Fleshing	Physical (CO <sub>2</sub> ) and chemical activation (KOH)	This study	17 mg/g	237.8 mg/g



**Fig. 12.** Schematic Cr (III) adsorption mechanism on the surface of activated carbon. a) Cr (III) interaction with carbonyl group. b) Cr (III) interaction with amino group.

material can have to be used as an adsorbent and be implemented in a circular economy using LIW as raw material for the adsorption of activated carbon.

### 3.8. Proposed adsorption mechanism

Cr (III) adsorption can be associated with the interaction of carboxylic groups and amines present in the organic matrix. In the case of Cr (VI), they are mainly associated with the hydroxyl group that interacts with the central ion of chromium VI.

Fig. 12 shows the possible interaction between the carbonyl and amino groups with Cr (III). Cr (III) species reported for the working pH (pH=5) are present as  $\text{Cr}(\text{OH})^{2+}$ ,  $\text{Cr}(\text{OH})_2^+$ ,  $\text{Cr}(\text{OH})_3^0$  [94]. These species interact with the amino,  $-\text{COO}-$ ,  $\text{C}=\text{O}$ , and  $\text{C}-\text{O}-\text{C}$  functional groups present on the surface of activated carbons (Zhao et al., 2023).

The carbonyl group can assist in the immobilization of chromium III by electrostatic attractive forces [94]. With the amino group, the electronegativity of the lone pair of nitrogen electrons and its weakness to polarize is linked to the small atomic radii of Cr (III) [95]. In addition, according to [96], Cr (III) ions bind with surface groups to form chelate complexes, ligands that connect with a single central atom considering that the coordination number for Cr (III) is 6.

Regarding Cr (VI), the adsorption is favored by acidic conditions [97]. At a pH equal to 5, the chromium VI species exist in equilibrium in the form of  $\text{HCrO}_4^-$  and  $\text{CrO}_7^{2-}$ . Equilibrium is written in Eqs. 10 and 11:



The excess of  $\text{H}^+$  ions can neutralize the surface of activated carbon negatively charged by the presence of hydroxyl groups and thus reduce

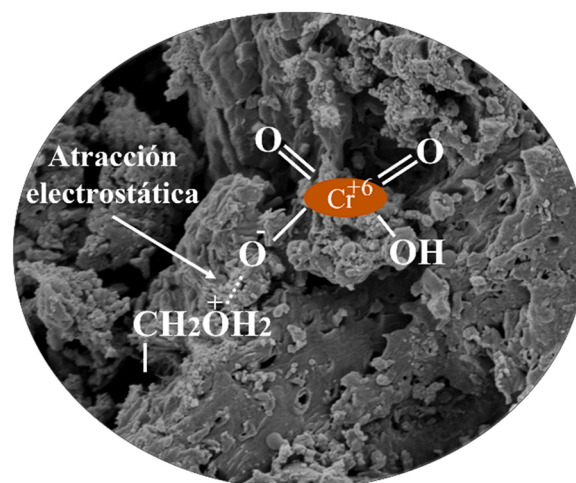


**Fig. 13.** Schematic mechanism of chromium VI adsorption on the surface of activated carbon.

the obstacle for dichromate ion diffusion [98]. The interaction of the Cr (VI) complexes with the hydroxyl groups on the surface of the activated carbons can form reversible reactions in equilibrium [99]. This may explain the decrease in the adsorption rate of Cr (VI) on activated carbons over time.

Fig. 13 shows the possible interaction between the hydroxyl groups present on the surface of activated carbons and the Cr (VI). This interaction is related to the electronic structure of the chromate anion according to the indicated reaction. After the elimination of oxygen from

the hydroxyl group present on the surface of the adsorbent, the interaction with chromium VI and its adsorption is carried out. Henryk et al., (\$year\$) [99].

#### 4. Conclusions

This paper presents a novel circular economy approach for using leather industry wastes as activated carbons to remove chromium from leather industry waste waters. Activated carbons were produced using chemical and physical activation from leather industry fleshing wastes. The highest mass yield obtained was 44.6% w/w using chemical activation at temperature of 500 °C and the KOH concentration of 3%. Cr (III) and Cr (VI) adsorption on the LIW activated carbons are exothermic. The adsorption process is spontaneous for Cr (III) while for Cr (VI) an external force is required to favour the adsorption process. The Freundlich and Temkin isotherm models presented the best fit compared to the Langmuir and DRK isotherm model in the adsorption of Cr (III). Maximum Cr (III) adsorption capacities above 202 mg/g were calculated with the Langmuir and DRK models. For Cr (VI) adsorption the DRK model presented the best fit with a maximum adsorption capacity equal to 41.6 mg/g. The adsorption of Cr (III) and Cr (VI) on activated carbon RQ4 followed a pseudo-second order kinetic model. The results obtained from adsorption demonstrate that activated carbon from LIW can be used for the removal of Cr (III) and Cr (VI) in the leather industry in Colombia. The surface groups that participate in the adsorption of Cr (III) are mainly the carbonyl and amino groups. For Cr (VI) adsorption, it was proposed that the protonated hydroxyl group interacts by electrostatic forces with the oxygen present in the negatively charged chromate ion.

#### CRedit authorship contribution statement

**Jennifer Jimenez-Paz:** Methodology, Investigation, Writing – original draft. **Juan José Lozada-Castro:** Resources, **Edward Lester:** Resources, **Orla Williams:** Writing – review & editing. **Lee Stevens,** Resources. **Juan Barraza-Burgos** Supervision, Writing – review & editing.

#### Declaration of Competing Interest

The authors declare that they have no known competing financial interests or personal relationships that could have appeared to influence the work reported in this paper.

#### Data Availability

Data will be made available on request.

#### Acknowledgements

This work was funded by CEIBA - Nariño Foundation for sponsoring the scholarship given to Jennifer Jiménez, to carry out doctoral studies in the Chemical Engineering Program of the Universidad del Valle, Cali, Colombia, as well as the Royal Academy of Engineering Industry Academia Partnership Programme [grant number IAPP1\100148] and the University of Nottingham Anne McLaren Fellowship. The authors would like to thank the University of Nottingham for the internship given to Jennifer Jiménez for the development of her research in the laboratories of the Department of Chemical and Environmental Engineering.

#### References

- [1] Y. Li, R. Guo, W. Lu, D. Zhu, Research progress on resource utilization of leather solid waste, *J. Leather Sci. Eng.* 1 (1) (2019) 1–17.
- [2] L. Wang, M. Chen, J. Li, Y. Jin, Y. Zhang, Y. Wang, A novel substitution-based method for effective leaching of chromium (III) from chromium-tanned leather waste: The thermodynamics, kinetics and mechanism studies, *Waste Manag.* 103 (2020) 276–284.
- [3] J. Kanagaraj, N.K. Chandra Babu, A.B. Mandal, Recovery and reuse of chromium from chrome tanning waste water aiming towards zero discharge of pollution, *J. Clean. Prod.* 16 (16) (2008) 1807–1813.
- [4] R.O. Oruko, R. Selvarajan, H.J.O. Ogola, J.N. Edokpayi, J.O. Odiyo, Contemporary and future direction of chromium tanning and management in sub Saharan Africa tanneries, *Process Saf. Environ. Prot.* 133 (2020) 369–386.
- [5] K. Chojnacka, D. Skrzypczak, K. Mikula, A. Witek-Krowiak, G. Izydorczyk, K. Kuligowski, P. Bandrów, M. Kulażyński, Progress in sustainable technologies of leather wastes valorization as solutions for the circular economy, *J. Clean. Prod.* 313 (May) (2021).
- [6] C.A. Forero-Núñez, J.A. Méndez-Velásquez, F.E. Sierra-Vargas, Energetic improvement of tanned leather solid wastes by thermal treatment, *Ing. Y. Desarro.* 33 (1) (2015) 1–17.
- [7] Y.S. Hedberg, Chromium and leather: a review on the chemistry of relevance for allergic contact dermatitis to chromium, *J. Leath. Sci. Eng.* 2 (2020) 1.
- [8] R. Aravindhan, B. Madhan, J.R. Rao, B.U. Nair, Recovery and reuse of chromium from tannery wastewaters using *Turbinaria ornata* seaweed, *J. Chem. Technol. Biotechnol.* 79 (11) (2004) 1251–1258, <https://doi.org/10.1002/jctb.1119>.
- [9] D.H. Cameron, G. McLaughlin, The adsorption nature of chrome tanning, *J. Phys. Chem.* 41 (7) (1937) 961–974.
- [10] P. Saranya, P. Bhavani, S. Swarnalatha, G. Sekaran, Biosequestration of chromium (III) in an aqueous solution using cationic and anionic biosurfactants produced from two different *Bacillus* sp. – a comparative study, *RSC Adv.* 5 (98) (2015) 80596–80611, <https://doi.org/10.1039/C5RA07999C>.
- [11] S. Famielec, Chromium concentrate recovery from solid tannery waste in a thermal process, *Materials* 13 (2020) 7.
- [12] V.J. Sundar, A. Gnanamani, C. Muralidharan, N.K. Chandrababu, A.B. Mandal, Recovery and utilization of proteinous wastes of leather making: a review, *Rev. Environ. Sci. Biotechnol.* 10 (2) (2011) 151–163.
- [13] C.B. Agustini, F. Spier, M. da Costa, M. Gutterres, Biogas production for anaerobic co-digestion of tannery solid wastes under presence and absence of the tanning agent, *Resour., Conserv. Recycl.* 130 (July 2017) (2018) 51–59.
- [14] T. Bhamra, R.J. Hernandez, Y. Rapitsenyane, R. Trimmingham, Product service systems: a sustainable design strategy for SMEs in the textiles and leather sectors, *She Ji* 4 (3) (2018) 229–248.
- [15] A. Wakeel, M. Xu, Y. Gan, Chromium-induced reactive oxygen species accumulation by altering the enzymatic antioxidant system and associated cytotoxic, genotoxic, ultrastructural, and photosynthetic changes in plants, *Int. J. Mol. Sci.* 21 (2020) 3.
- [16] P. cheng Lei, X. jiang Shen, Y. Li, M. Guo, M. Zhang, An improved implementable process for the synthesis of zeolite 4A from bauxite tailings and its Cr<sup>3+</sup> removal capacity, *Int. J. Miner., Metall. Mater.* 23 (7) (2016) 850–857.
- [17] M. Shahid, S. Shamsad, M. Rafiq, S. Khalid, I. Bibi, N.K. Niazi, C. Dumat, M. I. Rashid, Chromium speciation, bioavailability, uptake, toxicity and detoxification in soil-plant system: a review, *Chemosphere* 178 (2017) 513–533, <https://doi.org/10.1016/j.chemosphere.2017.03.074>.
- [18] I. Zinicovscaia, T. Mitina, T. Lupascu, G. Duca, M.V. Frontasyeva, O.A. Culicov, Study of chromium adsorption onto activated carbon, *Water, Air, Soil Pollut.* 225 (3) (2014) 1889, <https://doi.org/10.1007/s11270-014-1889-x>.
- [19] M.G. Arellano-Sánchez, C. Devouge-Boyer, M. Hubert-Roux, C. Afonso, M. Mignot, Quantitative extraction of chromium VI and III from tanned leather: a comparative study of pretreatment methods, *J. Leather Sci. Eng.* 3 (2021) 1.
- [20] N.K.C. Babu, K. Asma, A. Raghupathi, R. Venba, R. Ramesh, S. Sadulla, Screening of leather auxiliaries for their role in toxic hexavalent chromium formation in leather - posing potential health hazards to the users, *J. Clean. Prod.* 13 (12) (2005) 1189–1195.
- [21] S.S. Kahu, A. Shekhawat, D. Saravanan, R.M. Jugade, Two fold modified chitosan for enhanced adsorption of hexavalent chromium from simulated wastewater and industrial effluents, *Carbohydr. Polym.* 146 (2016) 264–273, <https://doi.org/10.1016/j.carbpol.2016.03.041>.
- [22] S. Langård, M. Costa, Chapter 33 - Chromium. In B. A. Fowler & M. B. T.-H. on the T. of M. (Fourth E. Nordberg (Eds)). *Handbook on the Toxicology of Metals* (Fourth, bl 717–742), Academic Press, 2015, <https://doi.org/10.1016/B978-0-444-59453-2.00033-0>.
- [23] M. Vasudevan, P.S. Ajithkumar, R.P. Singh, N. Natarajan, Mass transfer kinetics using two-site interface model for removal of Cr (VI) from aqueous solution with cassava peel and rubber tree bark as adsorbents 21 (2) (2016) 152–163.
- [24] G. Liu, R. Yu, T. Lan, Z. Liu, P. Zhang, R. Liang, Gallic acid-functionalized graphene hydrogel as adsorbent for removal of chromium (iii) and organic dye pollutants from tannery wastewater, *RSC Adv.* 9 (46) (2019) 27060–27068.
- [25] G. Tiravanti, D. Petruzzelli, R. Passino, Low and non waste technologies for metals recovery by reactive polymers, *Waste Manag.* 16 (7) (1996) 597–605.
- [26] M. Rosero, G. Taborda, G. Rodríguez, & Puerta, cristina nerin de la, Caracterización Quím. De. la Mater. orgánica Nat. Del. río Pasto *Quím. Ambient.* 35 (136) (2011) 363–370.
- [27] K. Reynolds, La calamidad del cromo VI, *Agua Latinoam.* 13 (2013) 5.
- [28] A. Rocha-Buevas, E. Trujillo-montalvo, C. Hidalgo-Patiño, Á. Hidalgo-Eraso, Carga de cáncer del departamento de Nariño y subregiones, *Colomb. Rev. Fac. Nac. De. Salud Publica* 32 (3) (2014) 340–354.
- [29] M.A. Hashem, M.A. Momen, M. Hasan, M.S. Nur-A-Tomal, M.H.R. Sheikh, Chromium removal from tannery wastewater using *Syzygium cumini* bark adsorbent, *Int. J. Environ. Sci. Technol.* 16 (3) (2019) 1395–1404.

- [30] M. Nigam, S. Rajoriya, S. Rani Singh, P. Kumar, Adsorption of Cr (VI) ion from tannery wastewater on tea waste: Kinetics, equilibrium and thermodynamics studies, *J. Environ. Chem. Eng.* 7 (3) (2019), 103188.
- [31] M. Nur-E-Alam, M. Abu Sayid Mia, F. Ahmad, M. Mafizur Rahman, Adsorption of chromium (Cr) from tannery wastewater using low-cost spent tea leaves adsorbent, *Appl. Water Sci.* 8 (5) (2018) 1–7.
- [32] M. Kamaraj, N.R. Srinivasan, G. Assefa, A.T. Aduagna, M. Kebede, Facile development of sunlit ZnO nanoparticles-activated carbon hybrid from pernicious weed as an operative nano-adsorbent for removal of methylene blue and chromium from aqueous solution: extended application in tannery industrial wastewater, *Environ. Technol. Innov.* 17 (2020), 100540.
- [33] E.I. Ugwu, J.C. Agunwamba, A review on the applicability of activated carbon derived from plant biomass in adsorption of chromium, copper, and zinc from industrial wastewater, *Environ. Monit. Assess.* 192 (2020) 4.
- [34] T. Kopac, A. Toprak, Preparation of activated carbons from Zonguldak region coals by physical and chemical activations for hydrogen sorption, *Int. J. Hydrog. Energy* 32 (18) (2007) 5005–5014, <https://doi.org/10.1016/j.ijhydene.2007.08.002>.
- [35] A. Arami-Niya, W.M.A.W. Daud, F.S. Mjalli, Comparative study of the textural characteristics of oil palm shell activated carbon produced by chemical and physical activation for methane adsorption, *Chem. Eng. Res. Des.* 89 (6) (2011) 657–664, <https://doi.org/10.1016/j.cherd.2010.10.003>.
- [36] K. Kandasamy, K. Tharmalingam, S. Velusamy, Treatment of tannery effluent using sono catalytic reactor, *J. Water Process Eng.* 15 (2017) 72–77, <https://doi.org/10.1016/j.jpwe.2016.09.001>.
- [37] P. Logam, A. Kumbahan, *Remov. Heavy Met. Wastewater Using Date Palm. A Biosorbent: A Comp. Rev.* 47 (1) (2018) 35–49.
- [38] S. Elabbas, L. Mandi, F. Berrekhis, M.N. Pons, J.P. Leclerc, N. Ouazzani, Removal of Cr(III) from chrome tanning wastewater by adsorption using two natural carbonaceous materials: eggshell and powdered marble, *J. Environ. Manag.* 166 (2016) 589–595, <https://doi.org/10.1016/j.jenvman.2015.11.012>.
- [39] N.F. Fahim, B.N. Barsoum, A.E. Eid, M.S. Khalil, Removal of chromium(III) from tannery wastewater using activated carbon from sugar industrial waste, *J. Hazard. Mater.* 136 (2) (2006) 303–309, <https://doi.org/10.1016/j.jhazmat.2005.12.014>.
- [40] R. Fonseca, L. Giraldo, J.C. Moreno-Pirajan, Adsorción de Cr(III) desde solución acuosa sobre carbones activados obtenidos de residuos de Zea mays, *AFINIDAD LXXII 569* (2014) 31–36.
- [41] E.P. Kuncoro, T. Soedarti, T.W.C. Putranto, H. Darmokoeseoemo, N.R. Abadi, H. S. Kusuma, Characterization of a mixture of algae waste-bentonite used as adsorbent for the removal of Pb2+ from aqueous solution, *Data Brief.* 16 (2018) 908–913, <https://doi.org/10.1016/j.dib.2017.12.030>.
- [42] S.A. Sadeek, N.A. Negm, H.H.H. Hefni, M.M.A. Wahab, Metal adsorption by agricultural biosorbents: adsorption isotherm, kinetic and biosorbents chemical structures, *Int. J. Biol. Macromol.* 81 (2015) 400–409, <https://doi.org/10.1016/j.ijbiomac.2015.08.031>.
- [43] R.A. Khera, M. Iqbal, A. Ahmad, S.M. Hassan, A. Nazir, A. Kausar, H.S. Kusuma, J. Niasr, N. Masood, U. Younas, R. Nawaz, M.I. Khan, Kinetics and equilibrium studies of copper, zinc, and nickel ions adsorptive removal on to Archontophoenix alexandrae: conditions optimization by rsm, *Desalin. Water Treat.* 201 (2020) 289–300, <https://doi.org/10.5004/dwt.2020.25937>.
- [44] M. Al-Jabari, Kinetic models for adsorption on mineral particles comparison between Langmuir kinetics and mass transfer, *Environ. Technol. Innov.* 6 (2016) 27–37, <https://doi.org/10.1016/j.eti.2016.04.005>.
- [45] H. Chen, J. Dou, H. Xu, Removal of Cr(VI) ions by sewage sludge compost biomass from aqueous solutions: Reduction to Cr(III) and biosorption, *Appl. Surf. Sci.* 425 (2017) 728–735, <https://doi.org/10.1016/j.apsusc.2017.07.053>.
- [46] C.-G. Lee, S. Lee, J.-A. Park, C. Park, S.J. Lee, S.-B. Kim, B. An, S.-T. Yun, S.-H. Lee, J.-W. Choi, Removal of copper, nickel and chromium mixtures from metal plating wastewater by adsorption with modified carbon foam, *Chemosphere* 166 (2017) 203–211, <https://doi.org/10.1016/j.chemosphere.2016.09.093>.
- [47] A. Abdolali, H.H. Ngo, W. Guo, J.L. Zhou, J. Zhang, S. Liang, S.W. Chang, D. D. Nguyen, Y. Liu, Application of a breakthrough biosorbent for removing heavy metals from synthetic and real wastewaters in a lab – scale continuous A continuous fixed – bed study was carried out utilising a breakthrough biosorbent, *Bioresour. Technol.* (2017), <https://doi.org/10.1016/j.biortech.2017.01.016>.
- [48] R. Elangovan, L. Philip, K. Chandraraj, Biosorption of hexavalent and trivalent chromium by palm flower (*Borassus aethiopicum*), *Chem. Eng. J.* 141 (2008) 99–111, <https://doi.org/10.1016/j.cej.2007.10.026>.
- [49] V. Vinodhini, N. Das, Packed bed column studies on Cr (VI) removal from tannery wastewater by neem sawdust, *Desalination* 264 (1–2) (2010) 9–14, <https://doi.org/10.1016/j.desal.2010.06.073>.
- [50] A. Bhatnagar, M. Sillanpää, A. Witek-krowiak, Agricultural waste peels as versatile biomass for water purification – a review, *Chem. Eng. J.* 270 (2015) 244–271, <https://doi.org/10.1016/j.cej.2015.01.135>.
- [51] S. Rengaraj, S.H. Moon, R. Sivabalan, B. Arabindoo, V. Murugesan, Agricultural solid waste for the removal of organics: adsorption of phenol from water and wastewater by palm seed coat activated carbon, *Waste Manag.* 22 (5) (2002) 543–548.
- [52] L.C.A. Oliveira, M.C. Guerreiro, M. Gonçalves, D.Q.L. Oliveira, L.C.M. Costa, Preparation of activated carbon from leather waste: a new material containing small particle of chromium oxide, *Mater. Lett.* 62 (21–22) (2008) 3710–3712, <https://doi.org/10.1016/j.matlet.2008.04.064>.
- [53] M. Vidaurre-Arbizu, S. Pérez-Bou, A. Zuazua-Ros, C. Martín-Gómez, From the leather industry to building sector: Exploration of potential applications of discarded solid wastes, *J. Clean. Prod.* (2021) 291.
- [54] M. Louarrat, Removal of Chromium Cr(Vi) of tanning effluent with activated carbon from tannery solid wastes, *Am. J. Phys. Chem.* 6 (6) (2017) 103, <https://doi.org/10.11648/j.ajpc.20170606.11>.
- [55] I.C. Kantarli, J. Yanik, Activated carbon from leather shaving wastes and its application in removal of toxic materials, *J. Hazard. Mater.* 179 (1–3) (2010) 348–356, <https://doi.org/10.1016/j.jhazmat.2010.03.012>.
- [56] H. Ozgunay, S. Colak, M.M. Mutlu, F. Akyuz, Characterization of leather industry wastes, *Pol. J. Environ. Stud.* 16 (6) (2007) 867–873.
- [57] Y. Palani, R. Rao Jonnalagadda, N. Fathima Nishter, Adsorption on activated carbon derived from tannery fleshing waste: adsorption isotherms, thermodynamics, and kinetics, *Environ. Prog. Sustain. Energy* 36 (6) (2017) 1725–1733, <https://doi.org/10.1002/ep.12637>.
- [58] A.E. Ogungbenro, D.V. Quang, K.A. Al-Ali, L.F. Vega, M.R.M. Abu-Zahra, Synthesis and characterization of activated carbon from biomass date seeds for carbon dioxide adsorption, *J. Environ. Chem. Eng.* 8 (5) (2020) 104–257, <https://doi.org/10.1016/j.jece.2020.104257>.
- [59] ASTM. (2018). D5373 - Standard Test Methods for Determination of Carbon, Hydrogen and Nitrogen in Analysis Samples of Coal and Carbon in Analysis Samples of Coal and Coke 1.
- [60] J. Jagiello, J.P. Olivier, Carbon slit pore model incorporating surface energetical heterogeneity and geometrical corrugation, *Adsorption* 19 (2–4) (2013) 777–783, <https://doi.org/10.1007/s10450-013-9517-4>.
- [61] E.P. Kuncoro, D.R.M. Isnadina, H. Darmokoeseoemo, O.R. Fauziah, H.S. Kusuma, Characterization, kinetic, and isotherm data for adsorption of Pb2+ from aqueous solution by adsorbent from mixture of bagasse-bentonite, *Data Brief.* 16 (2018) 622–629, <https://doi.org/10.1016/j.dib.2017.11.098>.
- [62] Y.A.B. Neolaka, G. Supriyanto, H. Darmokoeseoemo, H.S. Kusuma, Characterization, kinetic, and isotherm data for Cr(VI) removal from aqueous solution by Cr(VI)-imprinted poly(4-VP-co-MMA) supported on activated Indonesia (Ende-Flores) natural zeolite structure, *Data Brief.* 17 (2018) 969–979, <https://doi.org/10.1016/j.dib.2018.01.076>.
- [63] ASTM, A.S. for T. and M (2017). D1687 – 17: Standard Test Methods for Chromium in Water.
- [64] Y.A.B. Neolaka, Y. Lawa, J.N. Naat, A.A.P. Riwu, M. Iqbal, H. Darmokoeseoemo, H. S. Kusuma, The adsorption of Cr(VI) from water samples using graphene oxide-magnetic (GO-Fe3O4) synthesized from natural cellulose-based graphite (kesambi wood or Schleicher oleosa): Study of kinetics, isotherms and thermodynamics, *J. Mater. Res. Technol.* 9 (3) (2020) 6544–6556, <https://doi.org/10.1016/j.jmrt.2020.04.040>.
- [65] Y.A.B. Neolaka, Y. Lawa, J. Naat, A.A.P. Riwu, Y.E. Lindu, H. Darmokoeseoemo, B. A. Widiyaningrum, M. Iqbal, H.S. Kusuma, Evaluation of magnetic material IP@ GO-Fe3O4 based on Kesambi wood (Schleicher oleosa) as a potential adsorbent for the removal of Cr(VI) from aqueous solutions, *React. Funct. Polym.* 166 (April) (2021), 105000, <https://doi.org/10.1016/j.reactfunctpolym.2021.105000>.
- [66] C.F. De Almeida, R.C. De Andrade, G.F. De Oliveira, P.H. Suegama, E.J. De Arruda, J.A. Teixeira, C.T. De Carvalho, C.T. De Carvalho, Study of porosity and surface groups of activated carbons produced from alternative and renewable biomass: Buriti Petiole, Orbit - Electron. J. Chem. 9 (1) (2017) 18–26, <https://doi.org/10.17807/orbital.v9i1.878>.
- [67] J. Han, L. Zhang, B. Zhao, L. Qin, Y. Wang, F. Xing, The N-doped activated carbon derived from sugarcane bagasse for CO2 adsorption, *Ind. Crops Prod.* 128 (October 2018) (2019) 290–297.
- [68] J. Montalvo Andia, A. Larrea, J. Salcedo, J. Reyes, L. Lopez, L. Yokoyama, Synthesis and characterization of chemically activated carbon from *Passiflora ligularis*, *Inga feuillei* and native plants of South America, *J. Environ. Chem. Eng.* 8 (4) (2020), 103892, <https://doi.org/10.1016/j.jece.2020.103892>.
- [69] C. Su, Y. Guo, H. Chen, J. Zou, Z. Zeng, L. Li, VOCs adsorption of resin-based activated carbon and bamboo char: Porous characterization and nitrogen-doped effect, *Colloids Surf. A: Physicochem. Eng. Asp.* 601 (May) (2020), 124983, <https://doi.org/10.1016/j.colsurfa.2020.124983>.
- [70] A.F. Moreno-García, E.E. Neri-Torres, V.Y. Mena-Cervantes, R.H. Altamirano, G. Pineda-Flores, R. Luna-Sánchez, M. García-Solares, J. Vazquez-Arenas, J. K. Suastes-Rivas, Sustainable bio refinery associated with wastewater treatment of Cr (III) using a native microalgae consortium, *Fuel* 290 (January) (2021), <https://doi.org/10.1016/j.fuel.2020.119040>.
- [71] A.C. Gonçalves, H. Nacke, D. Schwantes, M.A. Campagnolo, A.J. Miola, C.R. T. Tarley, D.C. Dragunski, F.A.C. Suquila, Adsorption mechanism of chromium(III) using biosorbents of *Jatropha curcas* L, *Environ. Sci. Pollut. Res.* 24 (27) (2017) 21778–21790.
- [72] H.A. Murad, M. Ahmad, J. Bundschuh, Y. Hashimoto, M. Zhang, B. Sarkar, Y.S. Ok, A remediation approach to chromium-contaminated water and soil using engineered biochar derived from peanut shell, *Environ. Res.* 204 (PB) (2022), 112125, <https://doi.org/10.1016/j.envres.2021.112125>.
- [73] H. Chen, J. Dou, H. Xu, Removal of Cr(VI) ions by sewage sludge compost biomass from aqueous solutions: Reduction to Cr(III) and biosorption, *Appl. Surf. Sci.* 425 (2017) 728–735, <https://doi.org/10.1016/j.apsusc.2017.07.053>.
- [74] Y.A.B. Neolaka, G. Supriyanto, H.S. Kusuma, Adsorption performance of Cr(VI)-imprinted poly(4-VP-co-MMA) supported on activated Indonesia (Ende-Flores) natural zeolite structure for Cr(VI) removal from aqueous solution, *J. Environ. Chem. Eng.* 6 (2) (2018) 3436–3443, <https://doi.org/10.1016/j.jece.2018.04.053>.
- [75] M. Barkat, D. Nibou, S. Chegrouche, A. Mellah, Kinetics and thermodynamics studies of chromium(VI) ions adsorption onto activated carbon from aqueous solutions, *Chem. Eng. Process.: Process Intensif.* 48 (1) (2009) 38–47.
- [76] H. Demiral, I. Demiral, F. Tümsük, B. Karabacakoglu, Adsorption of chromium(VI) from aqueous solution by activated carbon derived from olive bagasse and

- applicability of different adsorption models, *Chem. Eng. J.* 144 (2) (2008) 188–196.
- [77] X. Song, Y. Zhang, C. Yan, W. Jiang, C. Chang, The Langmuir monolayer adsorption model of organic matter into effective pores in activated carbon, *J. Colloid Interface Sci.* 389 (1) (2013) 213–219.
- [78] F. Raposo, M. de La Rubia, R. Borja, Methylene blue number as useful indicator to evaluate the adsorptive capacity of granular activated carbon in batch mode: Influence of adsorbate/adsorbent mass ratio and particle size, *J. Hazard. Mater.*, 165(2009), 291–299 (2009), <https://doi.org/10.1016/j.jhazmat.2008.09.106>.
- [79] K.L. Martínez-Mendoza, J.M. Barraza-Burgos, N. Marriaga-Cabrales, F. Machuca-Martinez, M. Barajas, M. Romero, Production and characterization of activated carbon from coal for gold adsorption in cyanide solutions | Producción y caracterización de carbón activado a partir de carbón mineral para la adsorción de oro en soluciones cianuradas, *Ing. e Invest.* 40 (1) (2020) 34–44.
- [80] N. Ayawei, A.N. Ebelegi, D. Wankasi, Modelling and interpretation of adsorption isotherms, *J. Chem.* (2017) 2017.
- [81] Y.S. Ho, J.F. Porter, G. McKay, Equilibrium isotherm studies for the sorption of divalent metal ions onto peat: copper, Nickel and Lead single component systems, *Water, Air, Soil Pollut.* 141 (1–4) (2002) 1–33.
- [82] Y.A.B. Neolaka, Y. Lawa, J.N. Naat, A.A. Pau Riwu, H. Darmokoeseomo, G. Supriyanto, C.I. Holdsworth, A.N. Amenaghawon, H.S. Kusuma, A Cr(VI)-imprinted-poly(4-VP-co-EGDMA) sorbent prepared using precipitation polymerization and its application for selective adsorptive removal and solid phase extraction of Cr(VI) ions from electroplating industrial wastewater, *React. Funct. Polym.* 147 (December 2019) (2020), 104451, <https://doi.org/10.1016/j.reactfunctpolym.2019.104451>.
- [83] I.G.M.N. Budiana, J. Jasman, Y.A.B. Neolaka, A.A.P. Riwu, H. Elmsellem, H. Darmokoeseomo, H.S. Kusuma, Synthesis, characterization and application of cinnamoyl C-phenylcalix[4]resorcinarene (CCPCR) for removal of Cr(III) ion from the aquatic environment, *J. Mol. Liq.* 324 (2021), 114776, <https://doi.org/10.1016/j.molliq.2020.114776>.
- [84] S. Chen, Q. Yue, B. Gao, X. Xu, Equilibrium and kinetic adsorption study of the adsorptive removal of Cr(VI) using modified wheat residue, *J. Colloid Interface Sci.* 349 (1) (2010) 256–264, <https://doi.org/10.1016/j.jcis.2010.05.057>.
- [85] M.A.M. Lawrence, N.A. Davies, P.A. Edwards, M.G. Taylor, K. Simkiss, Can adsorption isotherms predict sediment bioavailability, *Chemosphere* 41 (7) (2000) 1091–1100, [https://doi.org/10.1016/S0045-6535\(99\)00559-7](https://doi.org/10.1016/S0045-6535(99)00559-7).
- [86] N. Pérez, J. González, L.A. Delgado, Estudio termodinámico del proceso de adsorción de iones de ni Y V por parte de ligninas precipitadas del licor negro kraft, *Rev. Latinoam. De. Metal. Y. Mater.* 31 (2) (2011) 168–181.
- [87] V. Yönten, N.K. Sanyürek, M.R. Kivanç, A thermodynamic and kinetic approach to adsorption of methyl orange from aqueous solution using a low cost activated carbon prepared from *Vitis vinifera* L, *Surf. Interfaces* 20 (February) (2020) 1–8, <https://doi.org/10.1016/j.surf.2020.100529>.
- [88] Y. Khambhaty, K. Mody, S. Basha, B. Jha, Kinetics, equilibrium and thermodynamic studies on biosorption of hexavalent chromium by dead fungal biomass of marine *Aspergillus niger*, *Chem. Eng. J.* 145 (3) (2009) 489–495, <https://doi.org/10.1016/j.cej.2008.05.002>.
- [89] P. Saha, S. Chowdhury, Insight Into Adsorption Thermodynamics, *Thermodynamics* (2011), <https://doi.org/10.5772/13474>.
- [90] M.L. Pinzón, L. Vera, Modeling of Cr (III) bioadsorption kinetics using orange peel, *Dyna* 76 (106) (2009) 95–106.
- [91] Y.J. Zhang, J.L. Ou, Z.K. Duan, Z.J. Xing, Y. Wang, Adsorption of Cr(VI) on bamboo bark-based activated carbon in the absence and presence of humic acid, *Colloids Surf. A: Physicochem. Eng. Asp.* 481 (2015) 108–116.
- [92] M.A. El-Nemr, I.M.A. Ismail, N.M. Abdelmonem, A. El Nemr, S. Ragab, Amination of biochar surface from watermelon peel for toxic chromium removal enhancement, *Chin. J. Chem. Eng.* 36 (2021) 199–222, <https://doi.org/10.1016/j.cjche.2020.08.020>.
- [93] A.El Nemr, Potential of pomegranate husk carbon for Cr(VI) removal from wastewater: kinetic and isotherm studies, *J. Hazard. Mater.* 161 (1) (2009) 132–141, <https://doi.org/10.1016/j.jhazmat.2008.03.093>.
- [94] B. Dash, S.K. Jena, S.S. Rath, Adsorption of Cr ( III) and Cr ( VI) ions on muscovite mica: experimental and molecular modeling studies, *J. Mol. Liq.* 357 (2022), 119116, <https://doi.org/10.1016/j.molliq.2022.119116>.
- [95] S. Fitri, A. Yahya, S. Ahmad, I. Sheikh, M. Ghazali, I. Fatimah, Surface Functionalized Halloysite with N-[3-(Trimethoxysilyl)Propyl] Ethylenediaminefor Chromium and Nickel Adsorption from Aqueous Solution, *Biointerf. Res. Appl. Chem.* 12 (6) (2022) 7205–7213.
- [96] B. Kaźmierczak, J. Molenda, M. Swat, Environmental Technology & Innovation The adsorption of chromium ( III) ions from water solutions on biocarbons obtained from plant waste, *Environ. Technol. Innov.* 23 (2021), 101737, <https://doi.org/10.1016/j.eti.2021.101737>.
- [97] N. Eggs, S. Salvarezza, R. Azario, N. Fernández, M. del C. García, Adsorción de cromo hexavalente en la cáscara de arroz modificada químicamente, *Av. En. Cienc. e Ing.* 3 (3) (2012) 141–151, [http://www.exeedu.com/publishing.cl/av\\_cienc\\_ing/2012/Vol3/Nro3/14-ACI1077-11-full.pdf](http://www.exeedu.com/publishing.cl/av_cienc_ing/2012/Vol3/Nro3/14-ACI1077-11-full.pdf).
- [98] V.O. Arief, K. Trilestari, J. Sunarso, N. Indraswati, S. Ismadji, Recent progress on biosorption of heavy metals from liquids using low cost biosorbents: characterization, biosorption parameters and mechanism studies, *Clean. - Soil, Air, Water* 36 (12) (2008) 937–962, <https://doi.org/10.1002/clen.200800167>.
- [99] K. Henryk, C. Jarosław, Z. Witold, Peat and coconut fiber as biofilters for chromium adsorption from contaminated wastewaters, *Environ. Sci. Pollut. Res.* 23 (1) (2016) 527–534, <https://doi.org/10.1007/s11356-015-5285-x>.